Zone folding effect in Raman *G*-band intensity of twisted bilayer graphene

Kentaro Sato,[1,*] Riichiro Saito,[1] Chunxiao Cong,[2] Ting Yu,[2,3] and Mildred S. Dresselhaus[4,5]

[1]*Department of Physics, Tohoku University, Sendai 980-8578, Japan*

[2]*Division of Physics and Applied Physics, School of Physical and Mathematical Sciences, Nanyang Technological University, Singapore 637371*

[3]*Department of Physics, Faculty of Science, National University of Singapore, Singapore 117542*

[4]*Department of Electrical Engineering and Computer Science, Massachusetts Institute of Technology, Cambridge, Massachusetts 02139-4037, USA*

[5]*Department of Physics, Massachusetts Institute of Technology, Cambridge, Massachusetts 02139-4307, USA*

The *G*-band Raman intensity is calculated for twisted bilayer graphene as a function of laser excitation energy based on the extended tight binding method. Here we explicitly consider the electron-photon and electron-phonon matrix elements of twisted bilayer graphene to calculate the resonance Raman intensity. The *G*-band Raman intensity is sensitive to the laser excitation energy and the twisting angle between the layers as a result of folding the electronic energy band structure. The Van Hove energy singularity, which is an electron transition energy between the conduction and valence bands, depends on $n - m$ of the twisting vector (n,m). The relative intensity of the *G* band as a function of twisting vectors is presented, which should be useful for the experimental identification of the twisting angle.

PACS number(s): 78.67.Wj, 78.30.−j, 73.22.Pr

I. INTRODUCTION

The physical properties of few-layer graphene depend on the number of graphene layers and its stacking structure. For example, the electronic band structure is highly sensitive to the structure of few-layer graphene,[1] and the AB Bernal stacked odd (even) layer number graphene has (does not have) linear energy bands near the Dirac point.[2,3] The optical conductance of trilayer ABA stacked graphene is observed to be higher than that of ABC stacked graphene.[4] Thus, it is important to reveal a relation between the crystal structure and the physical properties of few-layer graphene. In particular, since bilayer graphene can be constructed by folding monolayer graphene to overlap with the original graphene layer, we can generally make incommensurate bilayer graphene. Twisted bilayer graphene has been observed in the experimental studies of scanning tunneling microscope (STM) experiments[5,6] and in electron-diffraction studies in a transmission electron microscope (TEM).[7]

When the upper or lower layer of AB stacked bilayer graphene rotates about an axis perpendicular to the graphene surface, a super structure with a much larger unit cell than that of graphene appears at a specific rotation angle. Such a bilayer graphene is called twisted bilayer graphene, which has a unique electronic band structure.[8,9] The structure of twisted bilayer graphene has been observed experimentally as a Moiré pattern on the surface of graphite,[10–12] few-layer graphene,[13] and twisted bilayer graphene itself using STM[5,6] and Raman spectroscopy.[14–16] Several groups have shown that the Fermi velocity for twisted bilayer graphene decreases with decreasing rotation angle relative to that for monolayer graphene.[17–20] In order to utilize the twisted bilayer graphene in a semiconductor device, we need to know the rotation angle of twisted bilayer graphene for a large spatial region in a quick way compared with STM or TEM measurements.

Resonance Raman spectroscopy (RRS) has been used to study optical properties of graphene-related systems.[21] The resonance Raman spectra give us rich information to characterize not only the number of graphene layers but also the stacking order.[22] For example, the *G'* band intensity, its spectral width, and Raman shift tell us the number of graphene layers.[23] Recently, we found that the Raman shift and intensity of the *M* bands, which are relatively weak Raman peaks compared with the *G* and *G'* bands, appear in the range from 1700 cm^{-1} to 1800 cm^{-1} depending on the stacking order (ABA or ABC stacked) and the number of graphene layers.[4,24,25] Moreover, one of the *M* bands disappears in the spectra from incommensurate bilayer graphene (which is not AB stacked bilayer graphene) samples[24] because Raman active *M* bands are sensitive to the symmetry of bilayer graphene. The origin of some *M* bands are related to the motion of the out-of-plane transverse optical phonon mode. Since the electron energy dispersion relations of twisted bilayer graphene depend on the rotation angle, it is expected that a specific relevant behavior appears in the Raman spectra of twisted bilayer graphene. New Raman peaks were observed and discussed by using the double resonance Raman scattering process in the *D*-band region without disorder[14] and at 1435 and 1625 cm^{-1} for the given rotation angles 15° and 6°[15] in the Raman spectra of twisted bilayer graphene.

Recently, the strong *G*-band intensity enhancement of twisted bilayer graphene at a specific E_{laser} was reported.[7,26,27] It is considered that such a behavior gives us information to help evaluate the rotation angle of a twisted bilayer graphene sample using only resonance Raman spectroscopy. The purpose of this paper is to study the *G* band spectra of twisted bilayer graphene as a function of laser excitation energy (E_{laser}) and the rotation angle between the two graphene layers. In this paper, we calculate the *G* band Raman intensity of twisted bilayer graphene as a function of both E_{laser} and the twisting angle and we compare our calculations with experiments to find a relation between the rotation angle of a twisted bilayer graphene sample and E_{laser}. In Sec. II, the basic theory of twisted bilayer graphene and the calculation method are shown. In Sec. III, the calculated results are
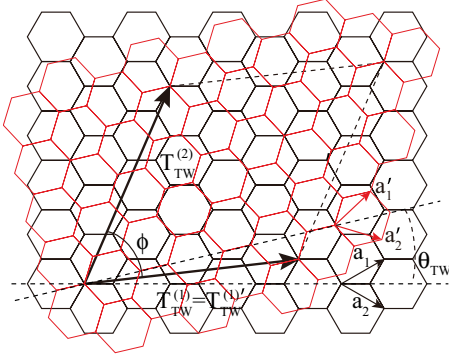
FIG. 1. (Color online) The unit cell for $(n,m) = (3,2)$ twisted bilayer graphene. Here, $t_1 = 3a_1 + 2a_2$, $t_2 = 5a_1 - 2a_2$, $t'_1 = 2a'_1 + 3a'_2$, $T = \sqrt{19}a$, $N = 76$, and $\theta_{TW} = 13.17°$. The second graphene layer (red) is rotated by θ_{TW} relative to AB stacking.

compared with experimental results. The summary is given in Sec. IV.

II. METHOD

The solution to define the periodic structure of a twisted bilayer graphene was discussed by several groups.[8,9,18–20,28,29] According to the previous work, we introduce a twisting vector to the first layer of a bilayer graphene lattice (black color in Fig. 1),

$$\boldsymbol{T}_{TW}^{(1)} = n\boldsymbol{a}_1 + m\boldsymbol{a}_2, \tag{1}$$

where n and m are integers ($0 < m < n$) such that $\gcd(n,m) = 1$ (gcd is an integer function of the greatest common divisor of two integers), $\boldsymbol{a}_1 = a(\sqrt{3}/2, 1/2)$ and $\boldsymbol{a}_2 = a(\sqrt{3}/2, -1/2)$ are the primitive lattice vectors for the first graphene layer, and $a = |\boldsymbol{a}_1| = |\boldsymbol{a}_2| = 0.246$ nm is the lattice constant of graphene. For simplicity, we assume that the two layers have a common origin. If there is a commensurate unit cell in the twisted bilayer graphene, another twisting vector $\boldsymbol{T}_{TW}^{(2)} = p\boldsymbol{a}_1 + q\boldsymbol{a}_2$ (p and q are integers) should appear in the first graphene layer. $\boldsymbol{T}_{TW}^{(2)}$ is obtained by rotating $\boldsymbol{T}_{TW}^{(1)}$ using a rotation matrix $R(\phi)$:

$$\begin{aligned}
\boldsymbol{T}_{TW}^{(2)} = p\boldsymbol{a}_1 + q\boldsymbol{a}_2 &= R(\phi)\boldsymbol{T}_{TW}^{(1)} \\
&= \left[n\cos\phi + (n+2m)\frac{\sin\phi}{\sqrt{3}}\right]\boldsymbol{a}_1 \\
&\quad + \left[m\cos\phi - (2n+m)\frac{\sin\phi}{\sqrt{3}}\right]\boldsymbol{a}_2,
\end{aligned} \tag{2}$$

where $R(\phi)$ is a rotation matrix for rotation by an angle ϕ around the axis that is perpendicular to the surface of the twisted bilayer graphene:

$$R(\phi) = \begin{pmatrix} \cos\phi & -\sin\phi \\ \sin\phi & \cos\phi \end{pmatrix}. \tag{3}$$

Here coefficients n, m, p, and q are integers used to construct a commensurate twisted bilayer graphene. ϕ is a multiple of $60°$ from Eq. (2). Without losing generality, we can select $\phi = 60°$. Thus, superlattice vectors $\boldsymbol{T}_{TW}^{(1)}$ and $\boldsymbol{T}_{TW}^{(2)}$ which define the unit

TABLE I. Possible pairs for (n',m') for a given (n,m) obeying $T < 10a$ by numerical calculation combined with $\cos(\theta_{TW})$, the twisting angle θ_{TW}, and the energy of the Van Hove singularity E_{11}. Some particularly interesting and exceptional solutions $[(n',m') \neq (m,n)]$ are listed. Corresponding E_{11} values (see below) are listed, too.

(n,m)	(n',m')	$\cos(\theta_{TW})$	θ_{TW}	E_{11} (eV)
(n,m)	(m,n)	Eq. (12)		Eq. (18)
(6,5)	(1,9)	161/182	27.80°	1.20
(5,3)	(0,7)	77/98	38.21°	1.57
(9,1)	(6,5)	169/182	21.79°	1.20
(9,1)	(5,6)	161/182	27.80°	1.20

cell of twisted bilayer graphene are given by

$$\boldsymbol{T}_{TW}^{(1)} = n\boldsymbol{a}_1 + m\boldsymbol{a}_2, \tag{4}$$

$$\boldsymbol{T}_{TW}^{(2)} = R(60°)\boldsymbol{T}_{TW}^{(1)} = (n+m)\boldsymbol{a}_1 - n\boldsymbol{a}_2. \tag{5}$$

The lattice constant T is given by

$$T = \left|\boldsymbol{T}_{TW}^{(1)}\right| = \left|\boldsymbol{T}_{TW}^{(2)}\right| = a\sqrt{n^2 + nm + m^2}. \tag{6}$$

The $\boldsymbol{T}_{TW}^{(1)}$ vector can also be described in the twisted second layer by using the primitive lattice vectors $\boldsymbol{a}'_1$ and $\boldsymbol{a}'_2$ and integers n' and m' for the second graphene layer (red color in Fig. 1),

$$\boldsymbol{T}_{TW}^{(1)'} = n'\boldsymbol{a}'_1 + m'\boldsymbol{a}'_2 = n'R(\theta_{TW})\boldsymbol{a}_1 + m'R(\theta_{TW})\boldsymbol{a}_2. \tag{7}$$

Here, we used the fact that $\boldsymbol{a}_i' = R(\theta_{TW})\boldsymbol{a}_i$ ($i = 1,2$) and θ_{TW} is the twisting angle between the two graphene layers. Since $|\boldsymbol{T}_{TW}^{(1)}| = |\boldsymbol{T}_{TW}^{(1)'}|$, we get

$$n^2 + nm + m^2 = n'^2 + n'm' + m'^2 \quad (n \neq n', m \neq m'). \tag{8}$$

The simplest solutions of Eq. (8) for (n',m') are $n' = m$ and $m' = n$. In Table I we list all possible (n',m') pairs for a given (n,m) obeying $T < 10a$ by numerical calculation. However, we found some exceptional properties for this solution. In Table I, we list some exceptional solutions for (n',m') which satisfy Eq. (8). For example we obtain $(n',m') = (0,7)$ for $(n,m) = (5,3)$. In order to obtain θ_{TW}, we use the fact $\boldsymbol{T}_{TW}^{(1)'} = \boldsymbol{T}_{TW}^{(1)}$ and from Eqs. (4) and (7), we get

$$n\boldsymbol{a}_1 + m\boldsymbol{a}_2 = n'R(\theta_{TW})\boldsymbol{a}_1 + m'R(\theta_{TW})\boldsymbol{a}_2. \tag{9}$$

From Eq. (9), the following simultaneous equations are derived:

$$\sqrt{3}(n'+m')\cos(\theta_{TW}) - (n'-m')\sin(\theta_{TW}) = \sqrt{3}(n+m),$$
$$\sqrt{3}(n'+m')\sin(\theta_{TW}) + (n'-m')\cos(\theta_{TW}) = n-m. \tag{10}$$

We multiply the first (second) equation of Eq. (10) by $\sqrt{3}(n' + m')$ $[(n' - m')]$ and add the two equations of Eq. (10) to obtain

$$\cos(\theta_{TW}) = \frac{nm' + n'm + 2(nn' + mm')}{2(n'^2 + n'm' + m'^2)}. \tag{11}$$

In the standard solution of Eq. (8) given by $n' = m$ and $m' = n$, we get

$$\cos(\theta_{TW}) = \frac{n^2 + 4nm + m^2}{2(n^2 + nm + m^2)}. \tag{12}$$

Here $\theta_{TW} = 0°$ (60°) corresponds to AB (AA) stacked bilayer graphene. It is noted that for the commensurate lattice the

rotation axis can be taken through an atom which is overlapped for the two layers. In Fig. 1 the number N of carbon atoms in the unit cell of twisted bilayer graphene is given by

$$N = 4\frac{|\boldsymbol{T}_{\mathrm{TW}}^{(1)} \times \boldsymbol{T}_{\mathrm{TW}}^{(2)}|}{|\boldsymbol{a}_1 \times \boldsymbol{a}_2|} = 4(n^2 + nm + m^2). \quad (13)$$

For example, Fig. 1 shows the unit cell for $(n,m) = (3,2)$ twisted bilayer graphene. Using Eqs. (6), (12), and (13), we obtain $\theta_{\mathrm{TW}} = \cos^{-1}(37/38) = 13.17°$, $T = \sqrt{19}a$, and $N = 76$.

The reciprocal lattice vectors $\boldsymbol{g}_1$ and $\boldsymbol{g}_2$ of twisted bilayer graphene are given by

$$\boldsymbol{g}_1 = \frac{1}{n^2 + nm + m^2}[n\boldsymbol{b}_1 + (n+m)\boldsymbol{b}_2], \quad (14)$$

$$\boldsymbol{g}_2 = \frac{1}{n^2 + nm + m^2}[m\boldsymbol{b}_1 - n\boldsymbol{b}_2], \quad (15)$$

where $\boldsymbol{b}_1 = 2\pi/a(1/\sqrt{3}, 1)$ and $\boldsymbol{b}_2 = 2\pi/a(1/\sqrt{3}, -1)$ are the reciprocal lattice vectors of graphene. The vectors $\boldsymbol{b}_1$ and $\boldsymbol{b}_2$ can be expressed in terms of $\boldsymbol{g}_1$ and $\boldsymbol{g}_2$ as follows:

$$\begin{aligned} \boldsymbol{b}_1 &= m\boldsymbol{g}_1 - n\boldsymbol{g}_2 \\ \boldsymbol{b}_2 &= n\boldsymbol{g}_1 + (n+m)\boldsymbol{g}_2. \end{aligned} \quad (16)$$

The angle between $\boldsymbol{g}_1$ and $\boldsymbol{g}_2$ is $120°$. The K point of graphene $\boldsymbol{K}_{\mathrm{g}} = (2\boldsymbol{b}_1 + \boldsymbol{b}_2)/3 = [(2n+m)\boldsymbol{g}_1 + (n+2m)\boldsymbol{g}_2]/3$ is folded to either the Γ or K point of twisted bilayer graphene when $\mathrm{mod}(n-m,3) = 0$ or $\mathrm{mod}(n-m,3) = 1,2$, respectively. The M point of graphene $\boldsymbol{M}_{\mathrm{g}} = (\boldsymbol{b}_1 + \boldsymbol{b}_2)/2 = [(n+m)\boldsymbol{g}_1 + m\boldsymbol{g}_2]/2$ would be folded to the Γ point of twisted bilayer graphene if both n and m are even numbers. However, such a case should be excluded because in these cases $\gcd(n,m) = 2$ and a smaller unit cell can be taken. Thus, for any cases of (n,m), $\boldsymbol{M}_{\mathrm{g}}$ is folded to the M point of twisted bilayer graphene which is defined by $(\boldsymbol{g}_1 + \boldsymbol{g}_2)/2$, and so on. Here it is important to know the distance of the M points of twisted bilayer graphene from the Dirac points [K or Γ depending on $\mathrm{mod}(n-m,3)$ as shown above] in zone-folded k space, since we see a Van Hove singularity in the joint density of states near the M point of twisted bilayer graphene (see Fig. 2).

The electron energy dispersion for twisted bilayer graphene is calculated based on the extended tight binding method.[30,31] We adopt the tight binding parameters given by Porezag et al.[32] Since the transfer and overlap integral matrix elements between carbon atomic orbitals are given by a function of distance between the center atom and its neighbor carbon atoms, the transfer and overlap matrices can be calculated by using a commensurate twisted bilayer graphene structure. We have reported, in previous papers, the optical transition energy of single-wall carbon nanotubes (SWNTs),[33] the Raman intensity of few-layer graphene,[4,25] and the Raman intensity of the radial breathing mode of SWNTs[34] as calculated by the extended tight binding method and we have compared the calculation results with experiments quantitatively using the tight binding parameters.[4,25,33,34] In this paper, the tight binding parameters for the transfer integral matrix elements are multiplied by 1.19 to reproduce experimental results.[35] We assume that the interlayer distance of twisted bilayer graphene has a constant value of 0.38 nm for simplicity.[26]

For the calculation of the phonon energy dispersion and electron-phonon interaction, we use the force constant model to calculate the phonon frequencies and eigenvectors.[36,37] We assume that the interlayer interaction between different graphene layers of twisted bilayer graphene is negligibly small for the LO and iTO phonons at the Γ point, which are associated with the G band and are not so sensitive to θ_{TW} because the LO and iTO phonons are in-plane lattice vibration modes.[7] Moreover, the interlayer interactions for both in-plane and out-of-plane phonon modes are sufficiently weak and not sensitive to the stacking structure.[4,24,25,38] Thus, we can use the phonon frequencies and eigenvectors for monolayer graphene as an approximation to calculate the resonance Raman G-band intensity for twisted bilayer graphene for simplicity.

The resonance Raman intensity is given by

$$I(E_{\mathrm{laser}}, \omega) = \sum_j \left| \sum_a \frac{M_{\mathrm{elop}}(j,b)M_{\mathrm{elph}}(b,a)M_{\mathrm{elop}}(a,j)}{(E_{\mathrm{laser}} - E_{aj})(E_{\mathrm{laser}} - E_{aj} - \hbar\omega)} \right|^2, \quad (17)$$

where $E_{aj} = (E_a - E_j) + i\gamma$, and j, a, and b denote, respectively, the initial state, the excited state, and the scattered state of an electron, while E_{laser}, E_j, E_a, and $\hbar\omega$ denote the energies of the excitation light, the initial and excited energies of an electron, and the phonon energies, respectively. Here we assume that the broadening factor γ is a constant value 0.1 eV[23] independent of E_{laser}. M_{elop} is an electron-photon matrix element between the ground and excited states[39,40] and M_{elph} is an electron-phonon matrix element from the initial state to the final state coupled by the G-band phonon.[41–43]
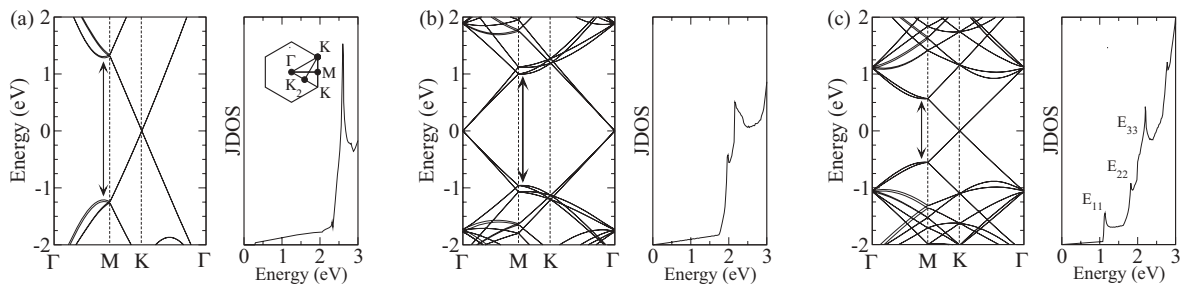

FIG. 2. The energy bands (left) and the joint density of states (right) (JDOS) for (a) (3,2), (b) (7,4), and (c) (7,5) twisted bilayer graphene. The joint density of states becomes large around the M points due to the band folding effect discussed in this paper. In the case of (7,4) twisted bilayer graphene, the $\boldsymbol{K}_{\mathrm{g}}$ point of graphene is folded to the Γ point of twisted bilayer graphene.

In this calculation we only consider a rotation about the axis which is perpendicular of the surface of the twisted bilayer graphene sample. Translation and other effects will be discussed elsewhere. We assume that the spectral width and Raman shift of the G band of twisted bilayer graphene does not depend on the twisting angle θ_{TW} in our calculation range.[7]

The Raman measurements were conducted by using a WITEC CRM200 Raman system with an objective of NA $= 0.95$ and a grating of 600 lines. The excitation laser lines of 633, 532, 488, and 457 nm were chosen. The twisting angle is measured by the optical microscope image of folded bilayer graphene.[26]

III. RESULTS AND DISCUSSION

Figure 2 shows the energy bands and joint density of states of [Fig. 2(a)] (3,2), [Fig. 2(b)] (7,4), and [Fig. 2(c)] (7,5) twisted bilayer graphene. From the energy band structure shown in Fig. 2, the joint density of states around the M points becomes large (arrows in Fig. 2) compared with that around the K points. Thus, it is expected that a strong optical absorption occurs around the M points in the folded Brillouin zone when E_{laser} is close to the energy separation between the π and π^* bands around the M points, which we call E_{11}. A strong optical absorption intensity therefore can be expected for a very small angle twisted bilayer graphene. However, for small θ_{TW}, in which the reduction of the Fermi velocity is significant, T (g_1 or g_2) becomes large (small), and, thus, E_{11} becomes much smaller than the energy of visual light and, thus, we can not observe any resonance Raman effect for small E_{11}.

In Fig. 3 we plot the G-band Raman intensity as a function of E_{laser} from 1.5 to 2.7 eV for [Fig. 3(a)] $(n,m) = (3,2)$ ($\theta_{TW} = 13.17°$) and [Fig. 3(b)] (4,3) ($\theta_{TW} = 9.43°$) twisted bilayer graphene, respectively. Circles denote the calculated G-band Raman intensities. In Fig. 3, the joint density of states is shown as the solid line. An enhancement in the G-band intensity occurs at the high joint density of states point due to the strong optical absorption intensity occurring in this E_{laser} range. Thus, we can point out that the origin of the G-band intensity enhancement of twisted bilayer graphene comes from the resonance around the M points of twisted bilayer graphene. The tendencies shown in the calculated
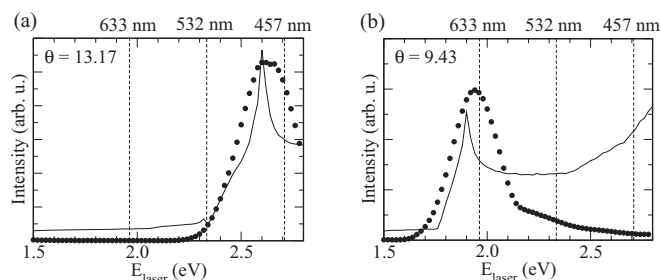

FIG. 4. (Color online) The energy separation at the Van Hove singularity point as a function of the twisted angle θ_{TW} of the twisted bilayer graphene. The data points for each family $n - m = $ const are connected by a line. The black, blue, and red symbols are mod($n - m$,3) $= 0$, mod($n - m$,3) $= 1$, and mod($n - m$,3) $= 2$, respectively. The circle and plus symbols denote E_{11} and E_{22}, respectively.

results agree well with the experimental results by Ni *et al.*[26] Very recently, Havener *et al.* reported the G-band Raman intensity as a function of θ_{TW} for given $E_{laser} = 2.33$ eV[27] and the maximum G-band intensity in their work corresponds to $\theta_{TW} = 12.5°$. We tentatively assign their twisting vector to (3,2) whose $\theta_{TW} = 13.17°$ and $E_{11} = 2.50$ eV. We also assign the data ($\theta_{TW} = 10.5°$ and $E_{laser} = 1.96$ eV) given by Kim *et al.*[7] to (7,5) whose data show $\theta_{TW} = 10.99°$ and $E_{22} = 1.91$ eV. Thus, the definition of the twisting vector is important for describing the twisted bilayer graphene. In terms of a characterization parameter the twisting vector is similar to the chiral vector (n,m) for single-wall carbon nanotubes.[44]

Figures 4 and 5, respectively, show the energy separation between the electronic energy bands at the Van Hove singularity point, E_{ii}, as a function of the twisting angle θ_{TW} and the lattice constant T of the twisted bilayer graphene. Here, the points corresponding to the family mod($n - m$,3) $= $ const and mod($n - m$,3) $= 0,1,2$ are each connected by a line in Figs. 4 and 5, respectively. The symbols are mod($n - m$,3) $= 0$ (black), mod($n - m$,3) $= 1$ (blue), and mod($n - m$,3) $= 2$ (red). E_{ii} increases with increasing θ_{TW} for the $n - m = $ const family and E_{ii} is inversely proportional to the lattice constant T due to the band folding effect. In the case of

FIG. 3. The calculated G-band intensity (circles) as a function of the laser excitation energy for (a) $(n,m) = (3,2)$ ($\theta_{TW} = 13.17°$) and (b) (4,3) ($\theta_{TW} = 9.43°$), respectively. The solid line denotes the joint density of states for each twisted bilayer graphene. The G-band intensity enhancement occurs at the singular point of the joint density of states vs energy curve in Fig. 2.
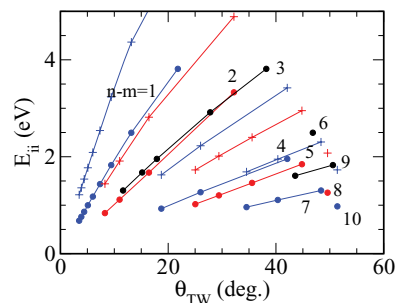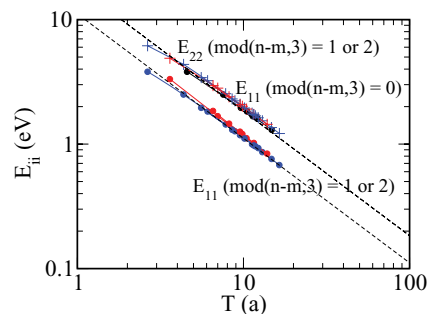

FIG. 5. (Color online) The energy separation at the Van Hove singularity point as a function of the lattice constant T of twisted bilayer graphene on a log-log scale. $a = 0.246$ nm is the lattice constant of graphene. Each family $n - m = $ constant is connected by a line. The black, blue, and red symbols are mod($n - m$,3) $= 0$, mod($n - m$,3) $= 1$, and mod($n - m$,3) $= 2$, respectively. The circle and plus symbols denote E_{11} and E_{22}, respectively.

mod$(n - m,3) = 1,2$, since the Dirac point of twisted bilayer graphene is at the K point, the energy separation is roughly proportional to the distance $|KM| = 2\pi/3T$ if we do not consider the effect of the reduction of the Fermi velocity[17–20] or the trigonal warping effect[45] in order to obtain a simple relation between E_{11} and T. On the other hand, in the case of mod$(n - m,3) = 0$, the K point of twisted bilayer graphene is folded to the Γ point because the K point is at $(2\boldsymbol{g}_1 + \boldsymbol{g}_2)/3$, as mentioned above. Thus, it is considered that the E_{11} energy is roughly proportional to the distance $|\Gamma M| = 2\pi/\sqrt{3}T$. Since we use the fact that $|\Gamma M| = \sqrt{3}|KM|$, there are two groups of points, namely mod$(n - m,3) = 0$ and mod$(n - m,3) = 1,2$, as shown in Fig. 5, for which the ratio of the E_{11} of mod$(n - m,3) = 0$ to that of mod$(n - m,3) = 1,2$ for a given lattice constant T is $\sqrt{3}$. If we use the linear energy dispersion $E(k) = \pm\sqrt{3}\gamma_0 ka/2$ of graphene to consider the energy dispersion of twisted bilayer graphene without the reduction of the Fermi velocity, then E_{11} is given by

$$E_{11} = \begin{cases} 2\pi\gamma_0 a/T & [\text{mod}(n - m,3) = 0] \\ 2\pi\gamma_0 a/\sqrt{3}T & (\text{others}) \end{cases}. \quad (18)$$

In Fig. 5, we plot the relation of Eq. (18) by dashed lines, in which we adopt the fitted value of $\gamma_0 = 2.92$ eV. The G-band Raman intensity enhancement occurs when choosing the energies in Figs. 4 and 5 for E_{laser} in the experiment.

Figure 6 shows the ratio of the experimental G-band Raman intensity for the twisted bilayer graphene I_G(TBLG) to that for graphene I_G(SLG) as a function of E_{laser}. The symbols are for the twisting angles $10.8°$ (star), $13°$ (triangle), and $25.3°$ (square), respectively, and follow the tentative assignment. The G-band intensity enhancement of $\theta_{\text{TW}} = 13°$ occurs for E_{laser} at 2.7 eV, which is consistent with the results of $(3,2)$ in Fig. 3(a). For the experimental results that $10.8°$ refer to, we can assign $(7,5)$ for (n,m). However the energy separation near the M point for $(7,5)$ is 1.12 eV which is much smaller than the experimental results at $E_{\text{laser}} = 2.32$ eV (532 nm) in Fig. 6. When we plot the energy dispersion and JDOS of $(7,5)$, we found the second (the third) peak, that we call E_{22} at 1.91 eV (E_{33} at 2.20 eV) as shown in Fig. 2(c). Thus, we conclude that the experimental results of $10.8°$ is $(n,m) = (7,5)$ and the enhancement occurs at E_{33}. The
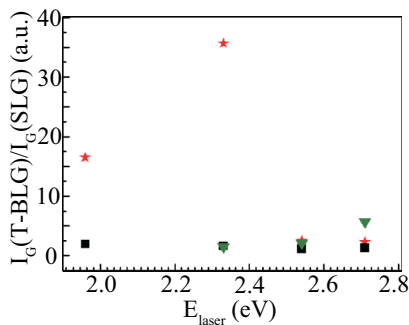
k point which gives E_{22} (E_{33}) for $(7,5)$ is located at the middle point K_2 along the Γ-K direction (near the Γ point), respectively. Since for the $|KK_2| = |KM|/\sqrt{3}$ relation in the folded Brillouin zone, the E_{22} energy for mod$(n - m,3) = 1,2$ twisted graphene appears at the same energy as E_{11} for mod$(n - m,3) = 0$ twisted bilayer graphene. In Fig. 5 we also plot E_{22} for mod$(n - m,3) = 1,2$ and we confirm that E_{22} for mod$(n - m,3) = 1,2$ twisted bilayer graphene appears in E_{11} for mod$(n - m,3) = 0$ graphene. E_{33} of $(7,5)$ is located near the Γ point, since $E_{33} \sim 2E_{11}$ which results from the fact $|K\Gamma| = 2|KM|$. For the result of $25.3°$ in Fig. 6, $(16,7)$ ($\theta_{\text{TW}} = 25.46°$) can be assigned. Here, the lattice constant of $(16,7)$ is $T = 20.42a$. If we consider a finite resonance window of the energy specified by γ in Eq. (17) to calculate the Raman intensity, the value of the joint density of states for the G-band Raman intensity enhancement decreases with increasing lattice constant T due to the band folding. Thus, it is expected that the G-band intensity enhancement effects for small twisting angles or for a large lattice constant T value is not strong compared with that for large twisting angles.

It is expected that the G-band Raman profile like Fig. 3 will help researchers to explain the experimental characterization of their sample to obtain a value for θ_{TW} from their measured Moiré patterns, since E_{11} depends not only on θ_{TW} but also on the lattice constant T. For a large T, we should consider the resonance effect of E_{22} which was observed in the case of $10.8°$ of Fig. 6. However, since the k point of E_{ii} ($i > 2$) is not near the M point in the Brillouin zone, the story becomes complicated. The detailed analysis of E_{22} for mod$(n - m,3) = 0$ and higher E_{ii} will be reported elsewhere.

Recently, Carozo *et al.* reported an experiment showing the Raman peaks at 1435 and 1625 cm^{-1} for the given twisting angles $15°$ and $6°$ and the theoretical analysis of the Raman shift and transition energy as a function of the twisting angle for the peaks to assign the twisting angle.[15] When we apply our analysis to these Raman peaks, it is expected that we observe the enhancement effect in the Raman profile for these peaks like the G-band Raman profile at the certain (n,m) and laser excitation energy within the resonance condition. Using their results, we tentatively assign their twisting vector $(5,4)$ whose $\theta_{\text{TW}} = 7.34°$ and $E_{22} = 2.54$ eV for their twisting angle $6°$. On the other hand, the resonance condition of the Raman peak (~ 7 eV) for their twisting angle $15°$ is too large for us to measure.[15] The detailed analysis will be reported in future work.

IV. SUMMARY

In this work, we calculated the G-band intensity of twisted bilayer graphene as a function of laser excitation energy. The G-band intensity enhancement of twisted bilayer graphene is shown to be related to its Van Hove singularity and to the joint density of states near the M point in the zone-folded Brillouin zone. The laser excitation energy at which the G-band intensity enhancement occurs for each twisting angle is found to decrease with decreasing twisting angle within the same $n - m$ family. The Van Hove singularity energy E_{ii} is inversely proportional to the length of the twisting vector. Moreover, E_{ii} depends on $n - m$ of the twisting vector (n,m).

FIG. 6. (Color online) Experimental results of the ratio of the G-band Raman intensity for the twisted bilayer graphene I_G(TBLG) to that for graphene I_G(SLG) as a function of E_{laser}. The symbols are for the twisting angles $10.8°$ (star), $13.0°$ (triangle), and $25.3°$ (square), respectively.

ACKNOWLEDGMENTS

*kentaro@flex.phys.tohoku.ac.jp

[1] S. Latil and L. Henrard, Phys. Rev. Lett. **97**, 036803 (2006).

[2] M. Koshino and T. Ando, Solid State Commun. **149**, 1123 (2009).

[3] M. Koshino, Phys. Rev. B **81**, 125304 (2010).

[4] C. Cong, T. Yu, K. Sato, J. Shang, R. Saito, G. F. Dresselhaus, and M. S. Dresselhaus, ACS Nano **5**, 8760 (2011).

[5] G. Li, A. Luican, J. M. B. Lopes dos Santos, A. H. Castro Neto, A. Reina, J. Kong, and E. Y. Andrei, Nat. Phys. **6**, 109 (2010).

[6] E. Sutter, D. P. Acharya, J. T. Sadowski, and P. Sutter, Appl. Phys. Lett. **94**, 133101 (2009).

[7] K. Kim, S. Coh, L. Z. Tan, W. Regan, J. M. Yuk, E. Chatterjee, M. F. Crommie, M. L. Cohen, S. G. Louie, and A. Zettl, Phys. Rev. Lett. **108**, 246103 (2012).

[8] J. M. B. Lopes dos Santos, N. M. R. Peres, and A. H. Castro Neto, Phys. Rev. Lett. **99**, 256802 (2007).

[9] E. J. Mele, Phys. Rev. B **81**, 161405 (2010).

[10] J. Xhie, K. Sattler, M. Ge, and N. Venkateswaran, Phys. Rev. B **47**, 15835 (1993).

[11] Z. Y. Rong and P. Kuiper, Phys. Rev. B **48**, 17427 (1993).

[12] M. Kuwabara, D. R. Clarke, and D. A. Smith, Appl. Phys. Lett. **56**, 2396 (1990).

[13] F. Varchon, P. Mallet, L. Magaud, and J.-Y. Veuillen, Phys. Rev. B **77**, 165415 (2008).

[14] A. K. Gupta, Y. Tang, V. H. Crespi, and P. C. Eklund, Phys. Rev. B **82**, 241406 (2010).

[15] V. Carozo, C. M. Almeida, E. H. M. Ferreira, L. G. Cançado, C. A. Achete, and A. Jorio, Nano Lett. **11**, 4527 (2011).

[16] A. Righi, S. D. Costa, H. Chacham, C. Fantini, P. Venezuela, C. Magnuson, L. Colombo, W. S. Bacsa, R. S. Ruoff, and M. A. Pimenta, Phys. Rev. B **84**, 241409 (2011).

[17] Z. Ni, Y. Wang, T. Yu, Y. You, and Z. Shen, Phys. Rev. B **77**, 235403 (2008).

[18] S. Shallcross, S. Sharma, E. Kandelaki, and O. A. Pankratov, Phys. Rev. B **81**, 165105 (2010).

[19] G. Trambly de Laissardiere, D. Mayou, and L. Magaud, Nano Lett. **10**, 804 (2010).

[20] E. Suárez Morell, J. D. Correa, P. Vargas, M. Pacheco, and Z. Barticevic, Phys. Rev. B **82**, 121407 (2010).

[21] A. Jorio, M. S. Dresselhaus, R. Saito, and G. Dresselhaus, *Raman Spectroscopy in Graphene Related Systems* (Wiley-VCH, Berlin, 2011).

[22] L. Malard, M. Pimenta, G. Dresselhaus, and M. Dresselhaus, Phys. Rep. **473**, 51 (2009).

[23] J. Park, A. Reina, R. Saito, J. Kong, G. Dresselhaus, and M. Dresselhaus, Carbon **47**, 1303 (2009).

[24] C. Cong, T. Yu, R. Saito, G. F. Dresselhaus, and M. S. Dresselhaus, ACS Nano **5**, 1600 (2011).

[25] K. Sato, J. S. Park, R. Saito, C. Cong, T. Yu, C. H. Lui, T. F. Heinz, G. Dresselhaus, and M. S. Dresselhaus, Phys. Rev. B **84**, 035419 (2011).

[26] Z. Ni, L. Liu, Y. Wang, Z. Zheng, L.-J. Li, T. Yu, and Z. Shen, Phys. Rev. B **80**, 125404 (2009).

[27] R. W. Havener, H. Zhuang, L. Brown, R. G. Hennig, and J. Park, Nano Lett. **12**, 3162 (2012).

[28] J. M. Carlsson, L. M. Ghiringhelli, and A. Fasolino, Phys. Rev. B **84**, 165423 (2011).

[29] P. Moon and M. Koshino, Phys. Rev. B **85**, 195458 (2012).

[30] V. N. Popov, New J. Phys. **6**, 17 (2004).

[31] G. G. Samsonidze, R. Saito, N. Kobayashi, A. Grüneis, J. Jiang, A. Jorio, S. G. Chou, G. Dresselhaus, and M. S. Dresselhaus, Appl. Phys. Lett. **85**, 5703 (2004).

[32] D. Porezag, T. Frauenheim, T. Köhler, G. Seifert, and R. Kaschner, Phys. Rev. B **51**, 12947 (1995).

[33] K. Sato, R. Saito, J. Jiang, G. Dresselhaus, and M. S. Dresselhaus, Phys. Rev. B **76**, 195446 (2007).

[34] K. Sato, R. Saito, A. R. Nugraha, and S. Maruyama, Chem. Phys. Lett. **497**, 94 (2010).

[35] A. Grüneis, C. Attaccalite, L. Wirtz, H. Shiozawa, R. Saito, T. Pichler, and A. Rubio, Phys. Rev. B **78**, 205425 (2008).

[36] R. Saito, G. Dresselhaus, and M. S. Dresselhaus, *Physical Properties of Carbon Nanotubes* (Imperial College Press, London, 1998).

[37] O. Dubay and G. Kresse, Phys. Rev. B **67**, 035401 (2003).

[38] R. Rao, R. Podila, R. Tsuchikawa, J. Katoch, D. Tishler, A. M. Rao, and M. Ishigami, ACS Nano **5**, 1594 (2011).

[39] A. Grüneis, R. Saito, G. G. Samsonidze, T. Kimura, M. A. Pimenta, A. Jorio, A. G. Souza Filho, G. Dresselhaus, and M. S. Dresselhaus, Phys. Rev. B **67**, 165402 (2003).

[40] J. Jiang, R. Saito, A. Grüneis, G. Dresselhaus, and M. S. Dresselhaus, Carbon **42**, 3169 (2004).

[41] J. Jiang, R. Saito, A. Grüneis, G. Dresselhaus, and M. S. Dresselhaus, Chem. Phys. Lett. **392**, 383 (2004).

[42] J. Jiang, R. Saito, G. G. Samsonidze, S. G. Chou, A. Jorio, G. Dresselhaus, and M. S. Dresselhaus, Phys. Rev. B **72**, 235408 (2005).

[43] G. G. Samsonidze, E. B. Barros, R. Saito, J. Jiang, G. Dresselhaus, and M. S. Dresselhaus, Phys. Rev. B **75**, 155420 (2007).

[44] R. Saito, M. Fujita, G. Dresselhaus, and M. S. Dresselhaus, Appl. Phys. Lett. **60**, 2204 (1992).

[45] R. Saito, G. Dresselhaus, and M. S. Dresselhaus, Phys. Rev. B **61**, 2981 (2000).